http://dx.doi.org/10.5935/0103-5053.20160124

J. Braz. Chem. Soc., Vol. 27, No. 12, 2290-2299, 2016.
Printed in Brazil - ©2016 Sociedade Brasileira de Química
0103 - 5053 $6.00+0.00

Article

A Mesoporous SiO_2/γ-Fe_2O_3/KI Heterogeneous Magnetic Catalyst for the Green Synthesis of Biodiesel

Alice L. Macedo,[a] José D. Fabris,[,a] Manoel J. M. Pires,[a] Wanessa L. Oliveira,[a] José D. Ardisson,[b] Rodinei Augusti,[c] Fermin H. Aragón,[b] Ricardo S. Santos,[a] Luiz C. A. Oliveira[c] and Márcio C. Pereira[d]*

[a]*Universidade Federal dos Vales do Jequitinhonha e Mucuri, UFVJM, 39100-000 Diamantina-MG, Brazil*

[b]*Centro de Desenvolvimento da Tecnologia Nuclear, CDTN/CNEN and* [c]*Departamento de Química, ICEx, Universidade Federal de Minas Gerais, Campus Pampulha, 31270-901 Belo Horizonte-MG, Brazil*

[d]*Instituto de Ciência, Engenharia e Tecnologia, Universidade Federal dos Vales do Jequitinhonha e Mucuri, UFVJM, 39803-371 Teófilo Otoni-MG, Brazil*

A magnetic catalyst (sample MCat) consisting of KI supported on a mixture of silica and maghemite (γ-Fe_2O_3) was prepared and used in the transesterification reaction for the synthesis of biodiesel. The energy dispersive X-ray spectrum of the catalyst showed signals due to Si, Fe, K, and I. Powder X-ray diffraction data revealed the amorphous nature of the SiO_2 and the duly impregnation of the support with KI. ^{57}Fe Mössbauer spectroscopy and magnetization measurements confirmed the ferrimagnetic iron oxide in the catalyst to be maghemite. N_2 adsorption-desorption data indicated that the silica is mesoporous with a specific area of 352 m^2 g^{-1}, enabling the impregnation of 40 and 11 wt.% of KI and maghemite, respectively, according to the chemical composition obtained by the X-ray fluorescence measurements. The MCat was found to be efficient in the transesterification reaction in the macaúba and soybean oils. The MCat was easily removed from the reaction medium, with a hand magnet, and efficiently reused for more four consecutive reaction cycles. The good catalytic activity along with its magnetic behavior, high chemical stability and recyclability make the MCat a suitable material for the green synthesis of biodiesel.

Keywords: biofuel, transesterification, heterogeneous catalyst, palm oil, soybean oil

Introduction

Optimizing chemical processes to produce liquid fuels (e.g., biodiesel and its derivatives) from renewable sources, as biomass, has been a scientific challenge directed to the development of new industrial technologies. A central topic is based on the enhancement of the industrial efficiency related to the chemical reactions of transesterification of triacylglycerols or esterification of free fatty acids to produce biodiesel.

The chemical efficiency of transesterification reactions of triacylglycerols with alcohol of short molecular chains (usually methanol or ethanol) requires an alkali catalyst. In such industrial processes, the most widely used are homogeneous catalysts based on alkaline compounds, usually potassium hydroxide.[1,2] Despite the high chemical efficiency of the homogeneous catalysts for the biodiesel production,[3] it has some drawbacks: (*i*) the hydroxide may react to saponify the free fatty acids and form alkaline carboxylates, which tend to decrease the primary reaction yields and hinder the full separation of the glycerol-rich by-product from the produced chemical mixture, and the subsequent purification of the fatty acid methyl esters;[4-6] (*ii*) the liquid medium containing the formed esters would also contain residual alkali, which is hardly separated from the industrial effluent,[7] and (*iii*) the catalyst cannot be further reused.[8] The technological development of highly active and selective heterogeneous catalysts for the industrial production of biodiesel is hence of great interest.

Solid catalysts having basic sites are chemically more efficient to such transesterification reactions than the catalysts with acid sites.[9] Xie and Li[10] have proposed an interesting approach by producing heterogeneous basic catalysts through the impregnation of KI onto a support

*e-mail: jdfabris@ufmg.br

(e.g., Al_2O_3) followed by thermal treatment at high temperatures (1000 °C) to activate the catalyst through the alleged formation of K_2O from the KI decomposition. Subsequent studies have reported a similar procedure to anchor KI onto silica[11] and alumina.[12-15] However, the method has the inconvenience of using extremely high temperatures to produce the catalysts, which may compromise the energy balance, in large-scale projects. Carvalho *et al.*[16] have used a basic heterogeneous catalyst consisting of a mixture of strontium compounds ($SrCO_3$, SrO, and $Sr(OH)_2$) for the transesterification of triacylglycerides in babassu and castor oils and their blends. They found biodiesel yields of 97.2, 96.4 and 95.3% from the babassu, castor oil, and 4:1 ratio babassu:castor oil blend, respectively. The use of heterogeneous catalysts for the biodiesel production reaction has several advantages in comparison with the homogeneous reaction: (*i*) the catalysts can be easily separated from the products, in order to be reused; (*ii*) the water-washing process and neutralization steps are much simpler; (*iii*) the contaminated water from the heterogeneous process are significantly reduced; (*iv*) the sewage treatment operations can be simplified and (*v*) the glycerol by-product is cleaner than that generated by the homogeneous process.[17-20] These features of the heterogeneous process have motivated scientific studies on the development of solid catalysts for transesterification reactions to produce fatty acid methyl esters (FAME) or fatty acid ethyl esters (FAEE).[21,22] However, heterogeneous catalysts have been found to present much lower chemical efficiency than the homogeneous alkalis and the activity loss of the catalyst is commonly associated the leaching of the active phase from the support.[23] Moreover, the leaching of the catalyst from the support and any extra cost to recover or to replace the catalyst are still issues to be taken into account.

A further prior challenge in developing processes for the biodiesel production consists of minimizing any harmful effect of the liquid effluents to the natural environment. This means designing heterogeneous magnetic catalysts in which the active chemical site would be sufficiently bound to a solid support, so to prevent the leaching to the liquid solution. Moreover, the magnetic catalyst could be recovered from the post-reaction medium and reused for several reaction cycles. This would reduce the number of steps of the industrial process and the proportion of disposal of wastes relatively to the strongly alkaline homogeneous process.

The impregnation of active catalysts and magnetic iron oxide onto inorganic supports are thought to be the key to the development of heterogeneous catalysts, for adding chemical efficiency, lowering the reaction time and streamlining processes of separation to reuse them in subsequent reaction cycles.[24,25] Magnetic catalysts have been reportedly applied in photocatalysis[26] and phase transfer catalysis.[27] Raita *et al.*[28] immobilized *Thermomyces lanuginosus* lipase in Fe_3O_4 to produce a biocatalyst showing high operational stability and ability to be magnetically separated and recycled for at least five consecutive batches, with chemical activity greater than 80%.

In this work, an active and recyclable heterogeneous magnetic catalyst was developed to produce biodiesel from the macaúba palm (*Acrocomia aculeata*) and soybean (*Glycine max*) oils. The heterogeneous catalyst (sample labeled as "MCat") was prepared using a high specific area support (amorphous silica, a-SiO_2), a basic catalyst (KI) to promote the transesterification reaction, and a magnetic component (maghemite, γ-Fe_2O_3), to make it easier the magnetic recovery of the catalyst from the liquid medium, after the reaction is completed.

Experimental

The bio-oil

The raw oil from the kernel of the macaúba (*Acronomia aculeata*) palm fruits was used as received from UBCM (commercial acronym for the Portuguese name "Unidade de Beneficiamento do Coco da Macaúba", which literally means "Processing Unit of Macaúba Nuts"), located in the city of Mirabela, state of Minas Gerais, Brazil. The kernel oil of the *Acronomia aculeata* fruit was subjected to physical and chemical analyses of acidity, saponification index, and peroxide value.

The soybean (*Glycine max*) oil was a commercial edible grade, with acid value < 0.4 mg KOH g^{-1} and saponification index of 185.6 mg KOH g^{-1}.

Materials synthesis

Preparation of the silica support

In a porcelain crucible, 4 g of silica-rich fine sand was mixed with 8 g sodium carbonate and the mixture was placed in a furnace at 800 °C for 4 h. The resulting material was transferred to a sintered plate filter and washed with boiling water. The aqueous solution (filtrate) was then acidified with hydrochloric acid down to pH 1 to the formation of a white and gelatinous precipitate, which was subsequently filtered through a sintered plate filter and washed with distilled water for several times to remove the foreign ions (e.g., sodium and chloride ions). Finally, the precipitate was dried in an oven at 150 °C to activate the surface of silica gel particles.[29]

Synthesis of the magnetic iron oxide nanoparticles

The magnetic iron oxide was obtained by co-precipitation of Fe^{2+} and Fe^{3+} in an alkaline medium followed by a complete spontaneous oxidation of Fe^{2+} to produce maghemite. Briefly, solutions of $FeCl_2$ and $FeCl_3$, with a stoichiometric ratio of 1:2 (Fe^{2+}/Fe^{3+}), were mixed, and the solution was kept under mechanical stirring at 60 °C in air atmosphere. Subsequently, a solution of ammonium hydroxide (18% v/v) was dripped into the mixture until pH 12 was reached. Then, the suspension containing the formed magnetite was cooled down to room temperature and centrifuged for 10 min at 3000 rpm. The supernatant was discarded, and the precipitate was washed with distilled water and again centrifuged.[30] The precipitate was then lyophilized, in order to obtain the maghemite nanoparticles.

Preparation of the magnetic heterogeneous catalyst

The heterogeneous catalyst was prepared from the a-SiO_2 support being impregnated with KI (to form catalytically active sites for the transesterification reaction) and magnetic iron oxide, for the purpose of facilitating the process of separation of the catalyst from the reaction medium. In short, the a-SiO_2 and the magnetic iron oxide were mixed at a mass ratio of 10:1. For each gram of this mixture, 20 mL of an aqueous solution of 35% KI were added. The material was sonicated for 25 min, filtered, and oven-dried at 150 °C in air for 2 h. Finally, the dried solid was calcined at 500 °C in an air atmosphere for 2 h to produce the magnetic catalyst (MCat). In this study, the temperature was kept at 500 °C to avoid the conversion of KI into K_2O at higher temperatures.[10] The MCat was stored in a desiccator until being directly used as a catalyst for the transesterification reaction.

Materials characterization

The morphology of the materials was investigated by scanning electron microscopy (SEM) using a tabletop SEM (Hitachi TM-3000). The energy dispersive X-ray spectroscopy (EDS) analysis was performed in a SwiftED3000 (Oxford Instruments) at 15 kV accelerating voltage. The crystallographic structures of the catalysts were assessed with powder X-ray diffraction (XRD) measurements, using a Shimadzu XRD 6000 diffractometer (CuKα radiation tube, λ = 1.541838 Å) equipped with a graphite monochromator. Scans were performed between 15 and 80° 2θ, with a scanning speed of 2° 2θ min^{-1}. Silicon was used as an external standard. Transmission ^{57}Fe Mössbauer spectra of the catalysts were collected under a constant acceleration regime of the ca. 25 mCi ^{57}Co/Rh gamma-ray source at 298 and 150 K by cooling the samples in a closed cycle He-cryostat. The spectra were least-squares-fitted with Lorentzian functions by using the software WinNormos™ for Igor. Isomer shift values were quoted relatively to the α-Fe foil. The magnetic hysteresis loops of the samples were measured with the samples at room temperature, using a Lakeshore vibrating sample magnetometer (VSM) model 7404. Surface areas were determined using the Brunauer-Emmett-Teller (BET) method with 22 point N_2 adsorption-desorption procedure in an Autosorb 1 Quantachrome gas sorption analyzer.

Transesterification reaction

The transesterification process to produce FAME was conducted at reflux with the one-necked round-bottom flask containing the reactants placed on a heating mantle under magnetic stirring. The conversion of triacylglycerols to esters of fatty acids was carried out with methanol:macaúba oil molar ratio of 30:1. The solid catalyst corresponded to 4.5 wt.% of the oil. The reactions were performed at 60 °C over a period of 8 h. After completion of the reaction, the solid catalyst was magnetically separated, and the liquid portion of the reacting medium was evaporated in a rotary evaporator to recover the methanol. The fractions containing esters and glycerin were placed in a phase separator funnel. The glycerol was removed, and the esters mixture was washed with distilled water and kept in a desiccator with magnesium sulfate as a desiccant material.

The products of the fatty acid methyl esters from the transesterification reaction were determined by gas chromatography (GC) coupled to a mass spectrometer (MS) using a GC-MS QP2010 Ultra (Shimadzu Corporation) instrument equipped with a fused silica capillary column Rxi-1ms (Restek Co.). The chemical structures of each eluting compound were assigned by comparing the experimental mass spectra with those of the NIST/EPA/NIH Mass Spectral Library (version 2.0) software, available in the GC-MS setup. The conversion of macaúba palm or soybean oil was calculated according to the Islam *et al.*[15] procedure.

Controlling experiments were further done with the single components of the magnetic heterogeneous catalysts, namely the sole silica gel and the maghemite samples. Specifically, the KI component was homogeneously mixed with the macaúba oil and methanol. All these controlling tests were performed under the same conditions as they were previously used for the magnetic catalyst.

Catalyst reusability

Catalyst reusability tests were performed by repeating the soybean oil transesterification over subsequent

extra cycles of reactions with 4.5 wt.% of the pre-used catalyst and molar ratio methanol:oil or 35:1. After the transesterification reaction had been completed, the catalyst was magnetically removed from the liquid medium, washed with methanol, dried at room temperature for 2 h to remove the moisture content and subsequently reused. The recycled catalyst was used under the same conditions, with soybean oil and methanol, for each reaction cycle. This same procedure was repeated for several reaction cycles in an attempt to evaluate the chemical stability of the catalyst.

Results and Discussion

Characterization of the catalysts

Figure 1 presents SEM images of the as-prepared amorphous silica powders before (Figure 1a) and after impregnation with KI and maghemite (γ-Fe_2O_3) to produce the MCat (Figure 1b). Both silica support itself and MCat were very similar in texture, as they exhibited sponge-like morphologies. The structure is formed by nano-sized silica particles linked together, resulting in a random arrangement of holes and cavities. The EDS spectrum of silica support (Figure 1c) contains signals belonging only to Si and O due to the SiO_2 support. In addition to O and Si signals, the EDS spectrum of MCat (Figure 1d) showed signs of K and I, suggesting that the KI was successfully impregnated on the silica support.

Figure 2 displays the powder XRD patterns of the prepared materials. Figure 2a revealed an extremely broad peak at approximately 2θ 15-35° due to amorphous structure of the silica support. The XRD pattern of the pure iron oxide (Figure 2b) showed characteristic Bragg reflections of a single phase corresponding to maghemite (γ-Fe_2O_3) (JCPDS card No. 4-755). Fitting the XRD pattern through the Rietveld algorithm led to an estimated value of the mean dimension of the maghemite cubic crystallographic cell of 8.3324(2) Å. The average coherent length of the maghemite crystallites, as determined by the Scherrer formula, was found to be 10 nm. The XRD pattern of the MCat (Figure 2c) is constituted of KI, which was identified by its sharp (111), (200), (220), (311), (222), (420) diffraction maxima, and a-SiO_2, as verified by a high background level in the range of 15-35° 2θ. The broad peak in the range of 30-40° 2θ, which superimposes the (220) reflection of KI, may be assigned to maghemite impregnated on the silica support.

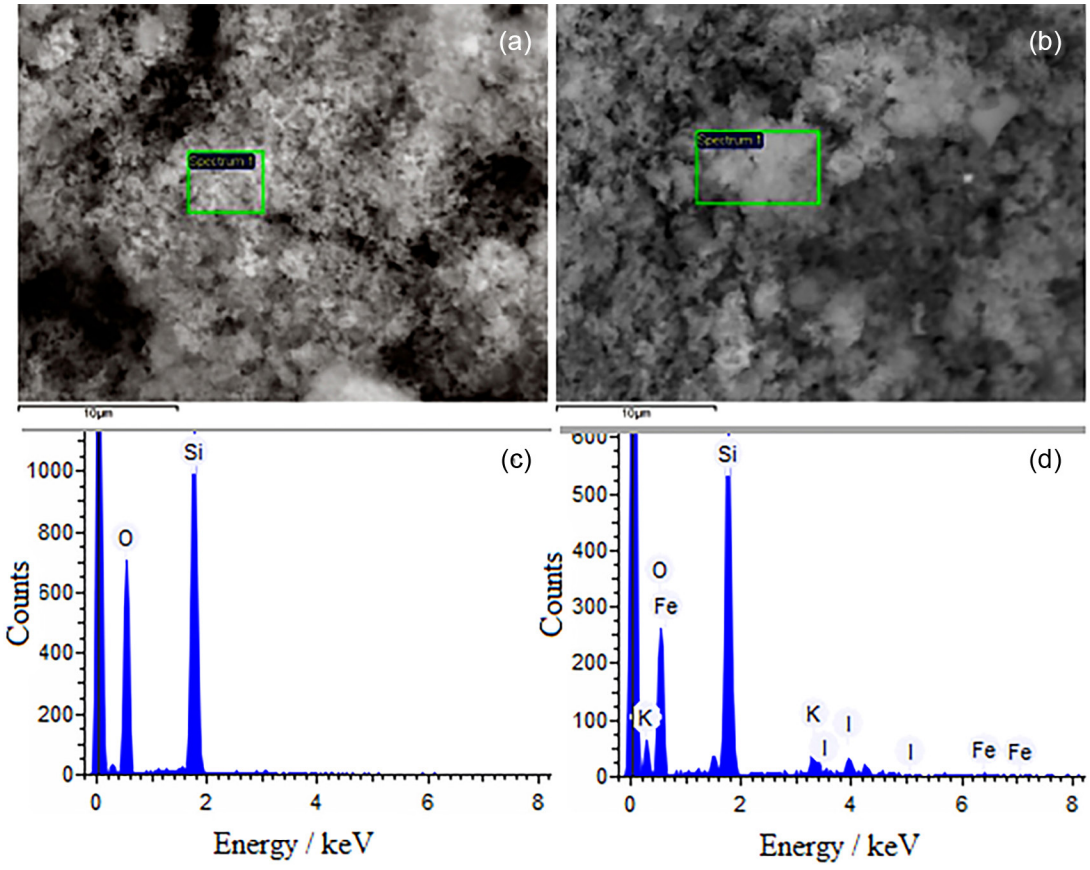

Figure 1. (a, b) SEM images; (c, d) EDS spectra of a-SiO_2 support and MCat, respectively.

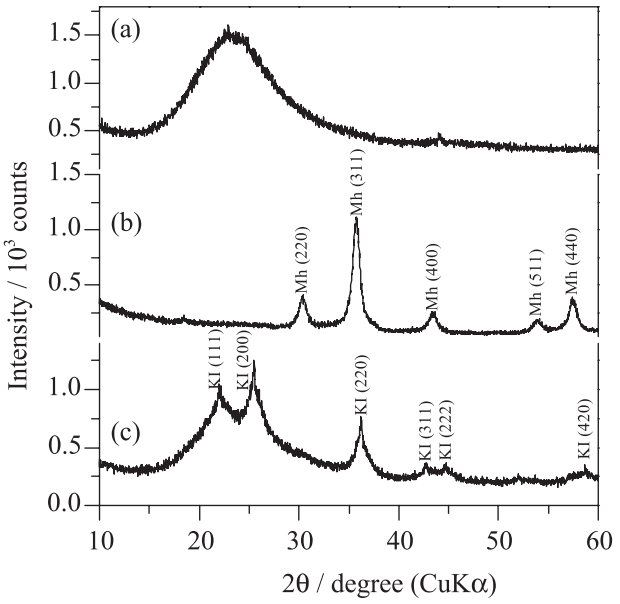

Figure 2. Powder XRD patterns of (a) a-SiO_2 support; (b) magnetic iron oxide; (c) MCat.

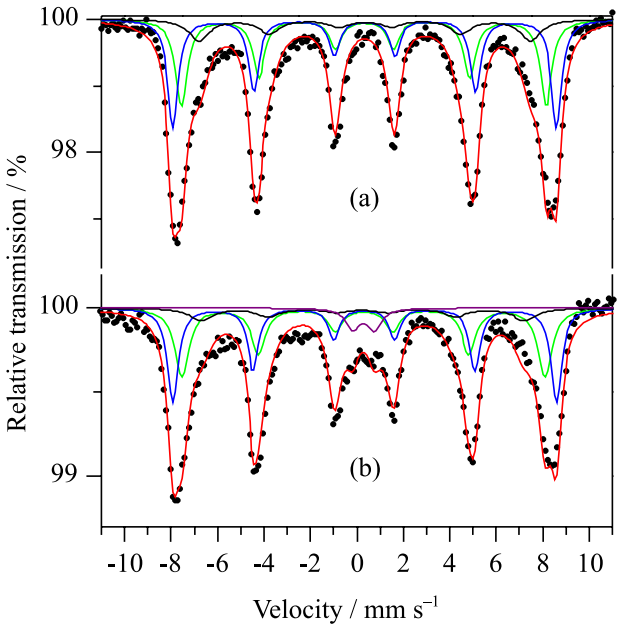

Figure 3. ^{57}Fe Mössbauer spectra of (a) pure iron oxide recorded at 298 K; (b) iron oxide and MCat recorded at 150 K.

^{57}Fe Mössbauer measurements at 298 and 150 K were performed in order to better characterize the magnetic iron oxide of the MCat. The experimental Mössbauer spectrum (Figure 3a) obtained for the iron oxide sample at 298 K is featured in a broad and asymmetric set of sextets of resonance lines, certainly reflecting an equally wide distribution of small particle sizes of the iron oxide undergoing different degrees of collective magnetic excitation,[31] according to the particle dimensions. The Mössbauer spectra of the pure iron oxide and MCat (Figure 3b) recorded at 150 K were fitted with three Lorentzian shaped sextets of resonance lines; the values of the fitted Mössbauer parameters are presented in Table 1.

Values of the isomer shift are characteristic of high-spin Fe^{3+} ions. For each of the two spectra, a sextet subspectrum (B_{hf} ca. 49 T, Table 1) was assigned to iron in tetrahedral coordination; the other subspectrum (B_{hf} ca. 51 T, Table 1) was due to Fe–O in the octahedral coordination environments of the spinel structure of the maghemite. A third subspectrum was fitted with a much lower value of hyperfine field ($B_{hf} < 44$ T, Table 1) and this may correspond to a fraction of still smaller particles of maghemite. In addition to those three sextets, the spectrum of this MCat sample shows a central doublet (ca. 6%), which is likely due to well-dispersed ultra-fine particles of maghemite experiencing superparamagnetic relaxation, which were spontaneously and selectively linked to the surface of the silica support.

Figure 4 shows the magnetic VSM hysteresis loops of pure iron oxide and MCat measured at 300 K. The saturation magnetization (M_s) was found to be

Table 1. Mössbauer parameters obtained from the fitting of the ^{57}Fe Mössbauer spectra recorded at 150 K

Sample	^{57}Fe site	Γ / (mm s^{-1})	δ / (mm s^{-1})	2ε or Δ / (mm s^{-1})	B_{hf} / T	RA / %
Iron oxide	[Fe^{3+}]	0.61(3)	0.41(4)	–0.02(1)	48.7(6)	37(1)
	{Fe^{3+}}	0.54(2)	0.45(4)	0.01(1)	51.2(5)	36(1)
	{Fe^{3+}}	1.06(6)	0.45(1)	–0.02(3)	44.2(2)	27(1)
MCat	[Fe^{3+}]	0.72(3)	0.39(6)	–0.02(1)	48.5(8)	41(1)
	{Fe^{3+}}	0.56(2)	0.45(1)	0.02(1)	51.2(6)	33(1)
	{Fe^{3+}}	1.19(9)	0.45(2)	0.04(1)	43.2(3)	20(1)
	Fe^{3+}	0.73[a]	0.45(1)	0.90(4)	–	6(2)

[a]Fixed value during numerical fitting convergence, parameter constrained to vary according to the least-squares convergence. Γ = resonance half-height line width; δ = isomer shift relative to αFe; Δ = quadrupole splitting; 2ε = quadrupole shift; B_{hf} = hyperfine magnetic field; RA = relative subspectral area; {Fe^{3+}} and [Fe^{3+}] = Fe^{3+} in octahedral and tetrahedral coordination sites of maghemite, respectively; numbers in parentheses are uncertainties over the last significant digit of the numerical value, as output by the least-squares-fitting computer program.

approximately 57 emu g^{-1} (Figure 4a), which is well consistent with the reported value for the pure nano-maghemite.[32] The M_s value of 4.6 emu g^{-1} for the MCat (Figure 4b) is correspondently lower, following the dilution of the maghemite in the silica matrix. Considering only the mass of maghemite in the sample MCat, it was found a Ms value of 41.8 emu g^{-1}, which is somewhat lower than that expected value for a pure maghemite (57 emu g^{-1}), more certainly due to the smaller crystallite size of the highly dispersed nanoparticles on the silica support of this sample. Both the coercivity and the remnant magnetization were found to be close to zero at 300 K. Because of its relatively high saturation magnetization, the MCat material can easily stick to a hand magnet, which makes it conveniently easier to separate and recover the catalyst from the liquid reaction medium.

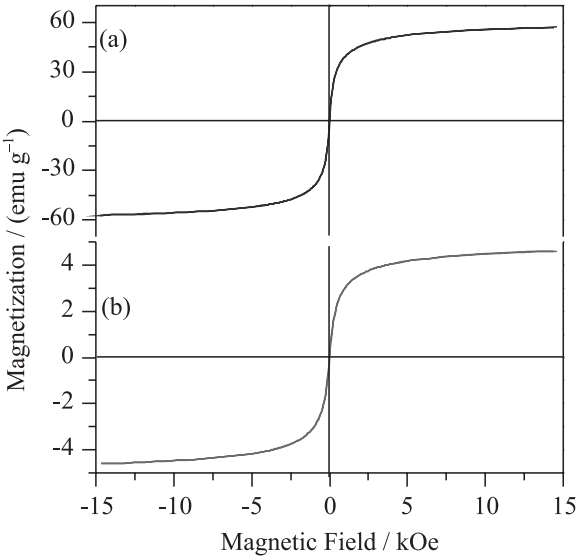

Figure 4. M-H curves of (a) pure iron oxide; (b) MCat recorded at 300 K.

The N_2 adsorption-desorption isotherms for the silica support, maghemite, and for this heterogeneous catalyst are shown in Figure 5a and the corresponding pore size distribution is shown in Figure 5b. All samples exhibited a type IV isotherm, which is typical of mesoporous materials (Figure 5b), with a type H4 hysteresis loop. The BET specific areas of the silica support, maghemite, and MCat were 352, 102, and 19 $m^2 g^{-1}$, respectively. It is worth to note that after impregnation of maghemite and KI on the silica support, occurred a significant decrease in the specific area of MCat, evidencing high efficiency of the incorporation of the catalyst and magnetic phase on the support.

Despite the fact that the incorporation of KI and maghemite on the silica support affects the specific area, the pore size distribution (Figure 5b) did not change; it remains in the mesoporous range of 90-490 Å in both a-SiO_2 and MCat samples.

Based on these findings, it is confirmed that this heterogeneous catalyst is constituted of three distinguished components: (*i*) amorphous SiO_2 with high specific area (352 $m^2 g^{-1}$) to serve as a support; (*ii*) the KI catalyst, a chemically useful Lewis base in the transesterification process, and (*iii*) maghemite, which is the magnetic component (M_s = 41.8 emu g^{-1}) that enables the separation and recovery of the catalyst for further reuse. The X-ray fluorescence (XRF) data indicated that the catalyst is composed of 49, 40 and 11 wt.% SiO_2, KI and Fe_2O_3, respectively.

Catalytic activity in transesterification reaction

The characterization data for this kernel macaúba oil were found to be: acid number, 2.16% FFA (free fatty acid); saponification number, 195 mg KOH g^{-1} and peroxide value, 35 mEq kg^{-1}.

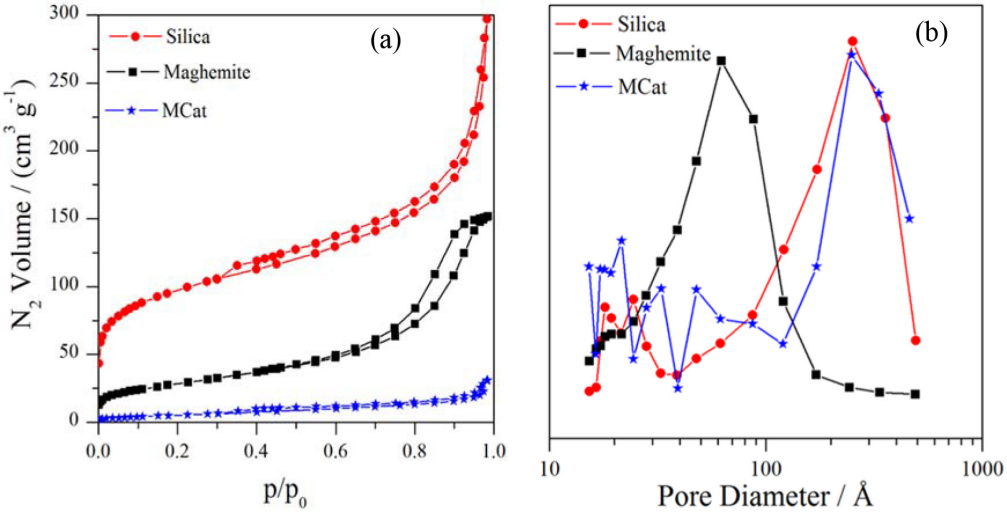

Figure 5. (a) N_2 adsorption-desorption isotherms; (b) pore size distribution.

The catalytic activity of MCat on the transesterification reaction was evaluated from the proportion of oil converted into methyl esters. An MCat-catalyzed conversion of 94.1% of the macaúba oil into biodiesel was achieved after 8 h reaction. To make more direct comparisons, the same reaction conditions were used for single component materials of (*i*) a-SiO_2; (*ii*) pure maghemite; (*iii*) unsupported (homogeneously, in the liquid solution) KI. It was noted that no significant conversion was individually attained for those single-component materials, even after 24 h reaction. However, it is worth mentioning that the homogeneous KI was active only under the catalyst concentration above 10 wt.% and methanol:oil molar ratio of 100:1; the corresponding reaction reached a total conversion of triacylglycerol into FAME in 8 h. These results suggest that the stabilization of KI on the silica support was an essential condition to produce a chemically active catalyst. Experiments with the soybean oil with MCat showed 94.4% conversion of the triacylglycerols into methyl esters after 1.5 h reaction.

The comparison of the FAME yields catalyzed with KI on different supports is provided in Table 2. These results evidence that, in this respect, the chemical effectiveness of the MCat is comparable to those reportedly found in other works (references in Table 2). Moreover, because of its magnetic features, the MCat has an advantage over the other catalysts showed in Table 2, in the sense that it can be magnetically removed from the liquid reaction medium, to be recovered and used for several subsequent reaction cycles for the biodiesel production. This is a remarkable characteristic if the material is, in a further development stage of the technology, envisaged to be used on an industrial scale, both from economic and environmental viewpoints. It must be observed that the MCat shows a still somewhat lower activity than that obtained with the homogeneous conventional process. Realistically, the MCat yields (esters in the final mixture: 94.4% for the soybean oil and 94.1% for the macaúba oil) approach well but still do not rigorously meet the recommended standard (96.5%, at minimum), as formally established by the Brazilian National Agency of Petroleum, Natural Gas and Biofuels (ANP, 2014).[33]

Catalyst reusability

The stability of MCat was evaluated by performing the reusability test of the catalyst. Figure 6 shows results of FAME yields on reusing the MCat catalyst. The amount of the biodiesel yields after the 4th consecutive cycle was higher than 90%, confirming that the MCat may be cyclically recovered and reused without significant loss of its catalytic activity.

Catalyst stability

The MCat was characterized by different techniques to evaluate its stability after the 4th reuse cycle. Figure 7a shows that the sponge-like morphology of MCat was

Table 2. Comparison of biodiesel yield catalyzed by KI supported on different matrices

Catalyst	KI loading / (wt.%)	Calcination		Reaction condition						Reuse catalyst		Reference
		Temperature / °C	time / h	Oil type	Reaction temperature / °C	Amount of catalyst (m/m oil) / %	Methanol:oil molar ratio	Reaction time / h	Biodiesel yield / %	Cycle	Biodiesel yield / %	
KI/γ-Al_2O_3	ca. 19.4	500	3	palm	60	4.0	14:1	4	98	11	79	15
CaO/KI/γ-Al_2O_3	35	650	4	palm	290	3.0	24:1	1	95	–	–	13
KI/oyster shells	ca. 16.6	300	2	soybean	60	3.5	6:1	4	85	3	85	34
KI/hydrotalcite/MgO	35	550	5	soybean	70	5.0	20:1	8	90	–	–	35
KI/m-SiO_2	15	600	3	soybean	70	5.0	16:1	8	90.1	–	–	11
KI/Al_2O_3	35	1071	3	soybean	60	2.5	15:1	8	96	–	–	10
KI/ZrO_2	35	1071	3	soybean	60	2.0	15:1	6	78.2	–	–	10
KI/ZnO	35	1071	3	soybean	60	2.0	15:1	6	72.6	–	–	10
KI/NaX	35	1071	3	soybean	60	2.0	15:1	6	12.9	–	–	10
KI/KL	35	1071	3	soybean	60	2.0	15:1	6	28.3	–	–	10
KI/Al_2O_3	35	1071	3	soybean	60	2.0	15:1	6	87.4	–	–	10
KI/γ-Fe_2O_3/a-SiO_2	40	500	1.5	soybean	60	4.5	35:1	1.5	94.4	4	> 90	this study
KI/γ-Fe_2O_3/a-SiO_2	40	500	1.5	macaúba palm	60	4.5	30:1	8	94.1	–	–	this study

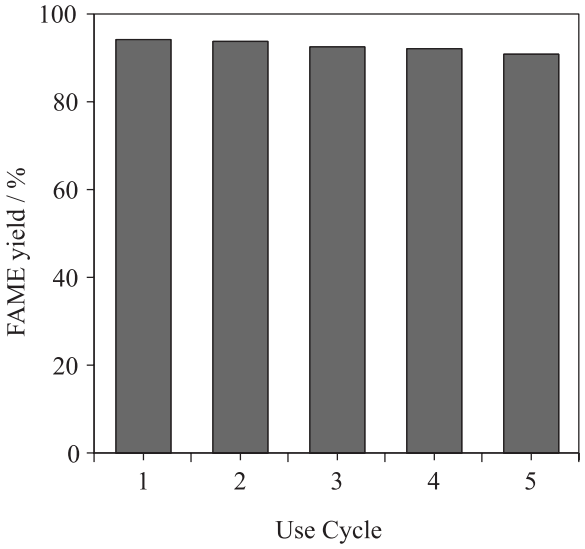

Figure 6. Reusability of MCat in the transesterification of soybean oil. Reaction conditions: methanol/oil molar ratio 35:1, catalyst loading 4 wt.%, reaction temperature 60 °C, reaction time 1.5 h.

not affected by the transesterification reaction. The EDX spectrum of the MCat material (Figure 7b) presented signals due to Si, O, K, and I, suggesting that even after the 4th reuse cycle the KI and Fe_2O_3 remain impregnated on the silica support. The chemical analysis indicated that less than 1 wt.% KI was leached from the MCat to the methanol-containing solution, after the 4th reuse cycle of the transesterification reaction: the catalyst was therefore chemically active for several cycles.

The XRD pattern (Figure 7c) shows Bragg reflections evidencing that both maghemite and KI were not significantly leached from the silica support. Moreover, K_2O or any other potassium compound was not detected by XRD, confirming that the KI active catalyst was indeed highly stable for at least 4 cycles of reuse.

Mössbauer spectra of MCat after reaction (Figure 8a) showed that maghemite was also stable under the experimental conditions used in the transesterification reaction. No difference between the spectra before and after reuse could be observed. Because of the high stability of the maghemite, its saturation magnetization value (4.3 emu g^{-1}) was maintained (Figure 8b, inset) after reusing of the catalyst. This is particularly attractive because the magnetic separation of the catalyst could be performed even after the 4th cycle of reaction.

Conclusions

A magnetic heterogeneous catalyst for the production of FAME biodiesel was successfully prepared by using an amorphous silica as a support, KI as the chemically active catalyst component, and maghemite, which itself allows the magnetic recovering of the catalyst after use. The catalyst promoted 94.1 and 94.4% chemical conversion of triacylglycerols in the macaúba palm and the soybean oil into FAME biodiesel, after 8 and 1.5 h reaction, respectively. These reaction times for the methylic transesterification of triacylglycerides in both, but particularly for the soybean oil, by using the magnetic heterogeneous catalyst, is reputed to be well favorably short, relatively to other known solid catalysts. Another remarkable characteristic is that KI and maghemite were intimately linked to the silica support, and this allows its magnetic separation and reuse for at least four additional

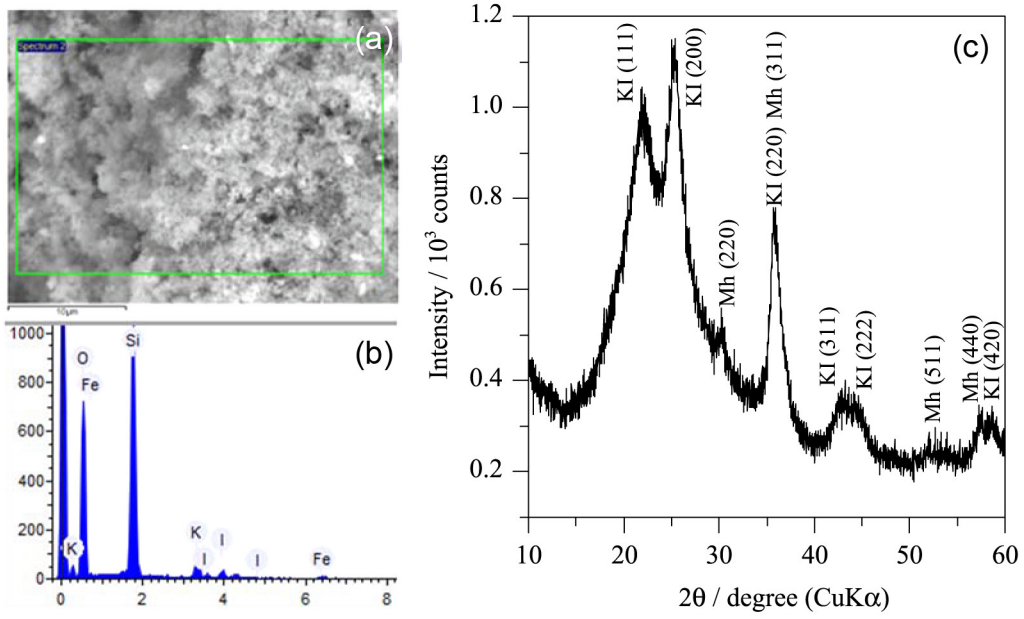

Figure 7. (a) SEM image; (b) EDX spectrum; (c) powder XRD pattern of MCat after the 4th cycle of reuse.

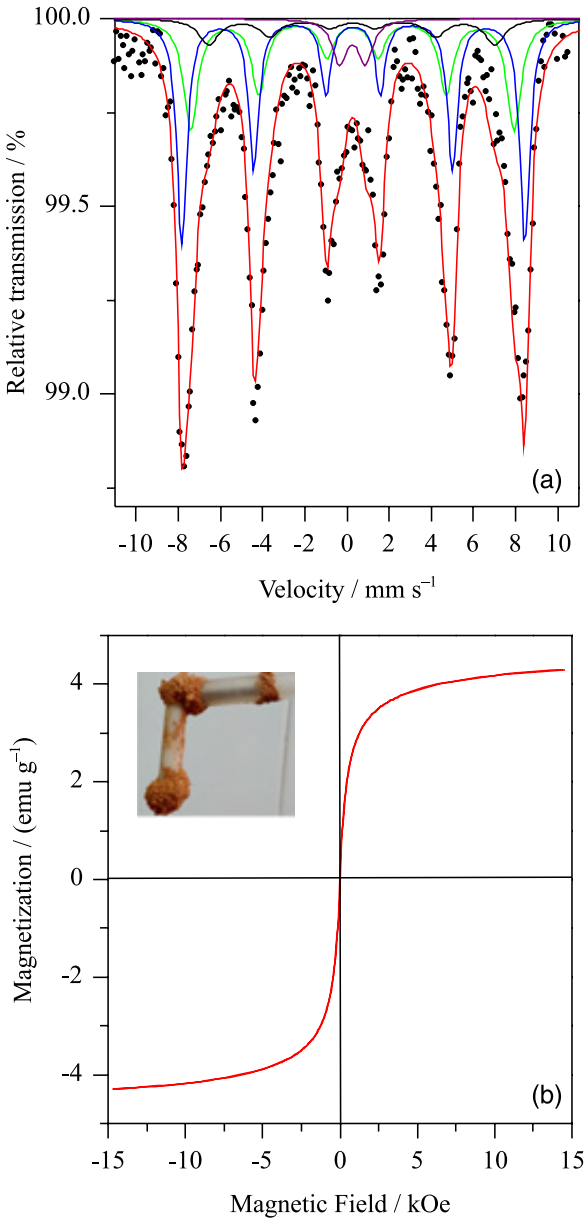

Figure 8. (a) 150 K Mössbauer spectra; (b) M-H curve of MCat after the 4th cycle of reuse.

subsequent cycles, to lead to FAME yields higher than 90%. The leaching of KI in the liquid reaction medium was found to be less than 1%, also making this recyclable catalyst very promising for being used in larger scale processes of the industrial production of biodiesel. It must be recognized that the FAME yields using the heterogeneous MCat do approach but still do not rigorously meet the recommended standard, as established by the Brazilian legislation, for the industrial production of biodiesel. More efforts are now being focused on further developments of the catalyst and of the corresponding conditions of the transesterification process, in a progressive attempt to fully reach those formal requirements.

Acknowledgments

This work was supported by FAPEMIG and CNPq (Brazil). A. L. M. thanks CAPES (Brazil) for sponsoring her DS studentship. J. D. F. is also indebted to CAPES for granting his visiting professorship at UFVJM under the PVNS program and to CNPq for the grant No. 305755-2013-7. The authors also thank José Joaquim Sá Teles (UFVJM) for his technical support in collecting the powder XRD and EDS data and Prof Edivaldo dos Santos Filho (UFVJM) for his help in collecting the 298 K-Mössbauer data.

References

1. Galvão, C. L. P. F.; Barbosa, M. N.; Araujo, A. S.; Fernandes Jr., V. J.; Santos, A. G. D.; Luz Jr., G. E.; *Quim. Nova* **2012**, *35*, 41.
2. Schuchardta, U.; Serchelia, R.; Vargas, R. M.; *J. Braz. Chem. Soc.* **1998**, *9*, 199.
3. Liew, W. H.; Hassim, M. H.; Ng, D. K. S.; *J. Cleaner Prod.* **2014**, *71*, 11.
4. Sharma, Y. C.; Singh, B.; *Renewable Sustainable Energy Rev.* **2009**, *13*, 1646.
5. Khan, T. M. Y.; Atabani, A. E.; Badruddin, I. A.; Badarudin, A.; Khayoon, M. S.; Triwahyono, S.; *Renewable Sustainable Energy Rev.* **2014**, *37*, 840.
6. Rincón, L. E.; Jaramillo, J. J.; Cardona, C. A.; *Renewable Energy* **2014**, *69*, 479.
7. Cordeiro, C. S.; Silva, F. R.; Wypych, F.; Ramos, L. P.; *Quim. Nova* **2011**, *34*, 477.
8. Gao, L.; Xu, B.; Xiao, G.; Lv, J.; *Energy Fuels* **2008**, *22*, 3531.
9. Borges, M. E.; Díaz, L.; *Renewable Sustainable Energy Rev.* **2012**, *16*, 2839.
10. Xie, W.; Li, H.; *J. Mol. Catal. A: Chem.* **2006**, *255*, 1.
11. Smart, C.; Sreetongkittikul, P.; Sookman, C.; *Fuel Process. Technol.* **2009**, *90*, 922.
12. Evangelista, J. P. C.; Chellappa, T.; Coriolano, A. C. F.; Fernandes Jr., V. J.; Souza, L. D.; Araujo, A. S.; *Fuel Process. Technol.* **2012**, *104*, 90.
13. Asri, N. P.; Machmudah, S.; Wahyudiono, S.; Budikarjono, K.; Roesyadi, A.; *Int. Chem. Eng. Process. Ind.* **2013**, *72*, 63.
14. Faria, E. A.; Marques, J. S.; Dias, I. M.; Andrade, R. D. A.; Suareza, P. A. Z.; Prado, A. G. S.; *J. Braz. Chem. Soc.* **2009**, *9*, 1732.
15. Islam, A.; Taufiq-Yap, Y. H.; Ravindra, P.; Teo, S. H.; Sivasangar, S.; Chan, E. S.; *Energy* **2015**, *89*, 965.
16. Carvalho, L. M. G.; Abreu, W. C.; Silva, M. G. O.; Lima, J. R. O.; Oliveira, J. E.; Matos, J. M. E.; Moura, C. V. R.; Moura, E. M.; *J. Braz. Chem. Soc*. **2013**, *24*, 550.
17. Diamantopoulos, N.; Panagiotaras, D.; Nikolopoulos, D.; *J. Thermodyn. Catal.* **2015**, *6*, 143.

18. Lee, A. F.; Bennett, J. A.; Manayil, J. C.; Wilson, K.; *Chem. Soc. Rev.* **2014**, *43*, 7887.
19. Chouhan, A. P. S.; Sarma, A. K.; *Renewable Sustainable Energy Rev.* **2011**, *15*, 4378.
20. Narasimharao, K.; Lee, A.; Wilson, K.; *J. Biobased Mater. Bioenergy* **2007**, *1*, 19.
21. Corma, A.; Garcia, H.; *Adv. Synth. Catal*. **2006**, *348*, 1391.
22. Zhou, G. X.; Chen, G. Y.; Yan, B. B.; *Biotechnol. Lett*. **2014**, *36*, 63.
23. Atadashi, I. M.; Aroua, M. K.; Aziz, A. R. A.; Sulaiman, N. M. N.; *J. Ind. Eng. Chem.* **2013**, *19*, 14.
24. Tang, S.; Wang, L.; Zhang, Y.; Li, S.; Tian, S.; Wang, B.; *Fuel Process. Technol*. **2012**, *95*, 84.
25. Rossi, L. M.; Costa, N. J. S.; Silva, F. P.; Wojcieszak, R.; *Green Chem.* **2014**, *16*, 2906.
26. Hu, S.; Guan, Y.; Wang, Y.; Han, H.; *Appl. Energy* **2011**, *88*, 2685.
27. Beydoun, D.; Amal, R.; Low, G. K. C.; McEvoy, S.; *J. Phys. Chem*. **2000**, *104*, 4387.
28. Raita, M.; Arnthong, J.; Champreda, V.; Laosiripojana, N.; *Fuel Process. Technol*. **2015**, *134*, 189.
29. Prado, A. G. S.; Faria, E. A; Padilha, P. M.; *Quim. Nova* **2005**, *28*, 544.
30. Laurent, S.; Forge, D.; Port, M.; Roch, A.; Robic, C.; Vander, E. L.; *Chem. Rev.* **2008**, *108*, 2064.
31. Mørup, S.; Frandsen, C.; Hansen, M. F.; *Beilstein J. Nanotechnol.* **2010**, *1*, 48.
32. Hwang, D. K.; Dendukuri, D.; Doyle, P. S.; *Lab Chip* **2008**, *8*, 1640.
33. Agência Nacional do Petróleo (ANP); Resolução No. 45 de 25 Agosto de 2014, *Especificação do Biodiesel Contida no Regulamento Técnico ANP No. 3/2014 e as Obrigações Quanto ao Controle da Qualidade a Serem Atendidas pelos Diversos Agentes Econômicos que Comercializam o Produto em Todo o Território Nacional*, publicada no Diário Oficial da União No. 163, 26 Agosto 2014, p. 68. http://pesquisa.in.gov.br/imprensa/jsp/visualiza/index.jsp?jornal=1&pagina=68&data=26/08/2014, accessed in April 2016.
34. Jairam, S.; Kolar, P.; Sharma, S. R. R.; Osborne, J. A.; Davis, J. P.; *Bioresour. Technol.* **2012**, *104*, 329.
35. Tantirungrotechai, J.; Chotmongkolsap, P.; Pohmakotr, M.; *Microporous Mesoporous Mat.* **2010**, *128*, 41.

Submitted: January 9, 2016
Published online: April 26, 2016